Bone cancer-induced pain is associated with glutamate signalling in peripheral sensory neurons

Yong Fang Zhu[1,2], Katja Linher-Melville[1,2] iD, Jianhan Wu[2], Jennifer Fazzari[2], Tanya Miladinovic[2] iD, Robert Ungard[1,2], Kan Lun Zhu[2], and Gurmit Singh[1,2]

Abstract

We previously identified that several cancer cell lines known to induce nociception in mouse models release glutamate in vitro. Although the mechanisms of glutamatergic signalling have been characterized primarily in the central nervous system, its importance in the peripheral nervous system has been recognized in various pathologies, including cancer pain. We therefore investigated the effect of glutamate on intracellular electrophysiological characteristics of peripheral sensory neurons in an immunocompetent rat model of cancer-induced pain based on surgical implantation of mammary rat metastasis tumour-1 cells into the distal epiphysis of the right femur. Behavioural evidence of nociception was detected using von Frey tactile assessment. Activity of sensory neurons was measured by intracellular electrophysiological recordings in vivo. Glutamate receptor expression at the mRNA level in relevant dorsal root ganglia was determined by reverse transcription polymerase chain reaction using rat-specific primers. Nociceptive and non-nociceptive mechanoreceptor neurons exhibiting changes in neural firing patterns associated with increased nociception due to the presence of a bone tumour rapidly responded to sulphasalazine injection, an agent that pharmacologically blocks non-vesicular glutamate release by inhibiting the activity of the system x_C^- antiporter. In addition, both types of mechanoreceptor neurons demonstrated excitation in response to intramuscular glutamate injection near the femoral head, which corresponds to the location of cancer cell injection to induce the bone cancer-induced pain model. Therefore, glutamatergic signalling contributes to cancer pain and may be a factor in peripheral sensitization and induced tactile hypersensitivity associated with bone cancer-induced pain.

Keywords

cancer-induced pain, neuropathic pain, electrophysiology, sensory neurons, dorsal root ganglion, bone metastasis, breast cancer cell, glutamate

Introduction

Bone cancer is associated with pathologic changes in bone turnover and severe skeletal pain, and changes in the mechanical hypersensitivity of skin have also been reported.[1] Preclinical studies utilizing rat bone cancer-induced pain (CIP) models have demonstrated significant glial, neuronal and inflammatory changes in the central nervous system (CNS) and peripheral nervous system (PNS).[2–4] In our previous CIP rat study, we reported that nociceptive high-threshold mechanoreceptor (HTM) as well as non-nociceptive low-threshold mechanoreceptor (LTM) neurons, including muscle spindle (MS) and cutaneous (CUT) neurons, showed plastic activity in dorsal root ganglia (DRG).[5,6] A possible explanation for peripheral changes in this neural

[1]Michael G. DeGroote Institute for Pain Research and Care, McMaster University, Hamilton, ON, Canada
[2]Department of Pathology and Molecular Medicine, McMaster University, Hamilton, ON, Canada

Corresponding Author:
Gurmit Singh, McMaster University, 1280 Main Street West, Hamilton, ON L8S4L8, Canada.
Email: singhg@mcmaster.ca

plasticity is that tumour growth induces nerve lesions, damaging the distal ends of nerve fibres normally innervating bone as well as those that innervate surrounding muscle and skin.

We previously showed that several human cancer cell lines that induce nociception in immunocompetent and syngeneic mouse models release glutamate via the system x_C^- cystine/glutamate antiporter in vitro.[7] System x_C^- is a non-vesicular membrane-bound transport mechanism that serves to exchange one molecule of intracellular glutamate for one molecule of extracellular cystine,[8] providing cancer cells a means to synthesize cysteine for optimally maintained redox balance. Exogenous glutamate released from peripheral bone tumours in the CIP model may then sensitize surrounding nerves, directly acting on adjacent nociceptors.[9–11] We therefore evaluated the effect of inhibiting system x_C^- in vivo in an immunocompromised mouse model of CIP, demonstrating that sulphasalazine (SSZ), an agent that blocks system x_C^- activity, induced a significant delay in the onset of nociception.[10] This finding suggested that glutamatergic signalling contributes to CIP.

Although the mechanisms of glutamatergic signalling have primarily been characterized centrally, evidence also supports a modulatory role for glutamate and its receptors in peripheral nociception and sensitization.[2,5,7,12,13] In animals, behavioural studies have demonstrated that the administration of glutamate[14–17] or glutamate agonists[18] evokes nociception. Locally injecting glutamate receptor antagonists attenuates formalin-,[19] carrageenan-,[16,20] Freund's complete adjuvant-[21] and interleukin-1β-[22] induced nocifensive responses and hyperalgesia/allodynia. In humans, subcutaneous glutamate injection into the skin, masseter muscle and trapezius muscles generated pain and mechanical allodynia,[12,23–25] with these effects being sensitive to NMDA antagonism.[24,26] This evidence suggests that the activation of peripheral glutamate receptors may contribute to nociception and peripheral sensitization in our CIP models.

In the current study, we specifically investigated the effect of glutamate on intracellular electrophysiological characteristics of peripheral sensory neurons to determine whether (1) glutamate injection near the head of the femur in a sham model (no live tumour cells present in the bone) induces neuronal excitation in relevant DRG similar to what we previously showed to be produced in response to the presence of a bone tumour using our syngeneic rat CIP model; and (2) neuronal excitability is altered in real time by acute in vivo SSZ injection near the site of the bone tumour in the rat CIP model. This work extends upon our previous findings that SSZ ameliorates bone CIP in mice and that there is plasticity in specific classes of neurons due to the presence of a bone tumour in rats, establishing a clear link between glutamate signalling and specific changes in peripheral nerve firing. We report that neurons in the sham model demonstrated excitation in response to glutamate injection, and the excitability of peripheral sensory neurons in the CIP model could be inhibited through local administration of SSZ. Furthermore, GluRs, including an ionotrophic NMDA receptor and two metabotropic GluRs (mGluRs), were shown to be expressed at the mRNA level in relevant DRG, providing a means to conduct glutamatergic signalling in the PNS. Our findings indicate that peripheral glutamate is involved in generating CIP and may contribute to peripheral sensitization and tumour-induced tactile hypersensitivity.

Methods

All experimental procedures conformed to the Guide to the Care and Use of Laboratory Animals, Vols. 1 and 2, of the Canadian Council on Animal Care, and all protocols were reviewed and approved by the McMaster University Animal Research Ethics Board.

Cell culture

Mammary rat metastasis tumour (MRMT)-1 cells were kindly provided by Dr. Philippe Sarret of the Université de Sherbrooke, Sherbrooke, QC. Cells were maintained in a humidified incubator at 37°C with 5% CO_2 in room air in RPMI 1640 (Life Technologies, Carlsbad, CA) supplemented with 10% fetal bovine serum and antibiotics (100 U ml^{-1} penicillin sodium and 1% antibiotic/antimycotic) (Life Technologies). MRMT-1 cells were verified to be free of mycoplasma contamination prior to experimental use.

Radiolabelled ^{14}C-cystine uptake assay

Cystine uptake is a surrogate measure of glutamate release and offers a more specific quantification of system x_C^- activity in vitro. Uptake of ^{14}C-cystine (0.5 μCi/ml; Perkin Elmer) was determined as described previously.[27] MRMT-1 cells were plated at a density of 1×10^5–2.5×10^5 cells per well in six-well plates 24 h prior to carrying out the uptake experiment. ^{14}C-cystine was diluted in Hank's Balanced Salt Solution (HBSS) containing each concentration of SSZ, ranging from 0 to 1000 μM or vehicle (DMSO). Cells were exposed to the SSZ/cystine mixture for 5 min at 37°C followed by washing with HBSS and lysis, as previously reported.[28] Samples were run in duplicate for three independent experiments. Scintillation counts per minute were normalized to total protein, which was determined using the Bradford assay.

Induction of the rat CIP model

Immunocompetent female Sprague-Dawley (SD) rats (Charles River Inc., St. Constant, QC) weighing 170–200 g were randomly assigned to CIP or sham (control) surgery groups. Rats were divided into three groups: one sham group (n = 6) and two CIP groups each consisting of n = 6 animals. Both CIP groups were induced by surgical implantation of rat MRMT-1 cells into the distal epiphysis of the right femur. The CIP-W2 group was examined at 14–16 days, and the CIP-W3 group was examined at >21 days post-MRMT-1 implantation. Rats were anaesthetised with inhaled isoflurane (3%–5% in O_2), and 3.0×10^4 MRMT-1 cells resuspended in 20 µL of HBSS were injected into the femur according to methods established by others.[5,17] Rats were oriented in a supine position with their right hind limb fixed to a stationary, convex support to maintain the limb in a flexed position. The limb was shaved and disinfected with chlorhexidine. A small incision was made on the medial side to expose the quadriceps femoris and the vests lateralis was incised to expose the medial epicondyle of the femur. A small cavity was drilled in between the medial epicondyle and the adductor tubercle with a 0.8 A stereotaxic drill equipped with a 1.75 mm burr. A 25-Ga needle was inserted into this cavity to penetrate the intramedullar canal. The needle was removed and replaced with a blunted 25-Ga needle attached to a Hamilton syringe containing either the live (CIP) or heat/freeze-inactivated (sham) MRMT-1 cell suspensions. Each respective suspension was slowly dispensed into the canal and left for 1 min to prevent leakage. The cavity was then sealed with dental amalgam and fixed using a curing light. The wound was flushed with sterile deionized water, and connective tissue and muscle were closed using a discontinuous suture pattern. Fascia and the subcutaneous skin layer were closed using a continuous suture. Finally, discontinuous sutures were used to close the outer layer of skin. The site was then cleaned with hydrogen peroxide.

Von Frey paw withdrawal threshold test

Behavioural tests were performed immediately prior to anaesthesia required for electrophysiological recordings to quantify the development of tactile hypersensitivity associated with CIP. Rats were placed in a transparent Plexiglas box with 0.5 cm diameter holes spaced 1.5 cm apart on the floor[13,14,21] to allow full access to the paw. Animals were habituated to the box until cage exploration and major grooming activities ceased. Von Frey filaments (Stoelting Co., Wood Dale, IL) were applied to the plantar surface of the ipsilateral hind paw to determine mechanical withdrawal thresholds using the up-down method.[29] A von Frey filament was applied five times for 3–4 s each at 3-s intervals to a different spot on the plantar surface of the hind paw. Filaments were applied in ascending order of force until a clear withdrawal response was observed. When this occurred, the next lightest filament was applied, and the process continued until a 50% withdrawal response threshold was achieved. Brisk foot withdrawal in response to the mechanical stimulus was interpreted as a valid response.

In vivo intracellular DRG recordings

Details of acute intracellular electrophysiological recording techniques have been reported previously in CIP models.[5,6,30,31] Briefly, each rat was initially anaesthetised via intraperitoneal delivery of a mixture of ketamine, xylazine and acepromazine. The right jugular vein was cannulated for intravenous drug infusion, and the rat was fixed in a stereotaxic frame with the vertebral column rigidly clamped at lumbar (L)2 and L6. The L4 DRG was selected for study, as it contains large numbers of hind leg afferent somata. A laminectomy was performed to expose the ipsilateral L4 DRG. The L4 dorsal root was sectioned close to the spinal cord and placed on a bipolar electrode (FHC, Bowdoinham, ME) used for stimulation. The exposed spinal cord and DRG were covered with paraffin oil at 37°C to prevent drying. A temperature-controlled infrared heating lamp was used to maintain rectal temperature at 37°C.

For all recordings, each rat was maintained at a surgical level of anaesthesia using sodium pentobarbital (20 mg/kg; Ceva Sante Animal, Libourne, France) and mechanically ventilated via a tracheal cannula using a Harvard Ventilator (Model 683, Harvard Apparatus, QC). The ventilation parameters were adjusted so that end-tidal CO_2 concentration was maintained at 40–50 mmHg (CapStar-100 End-Tidal CO_2 analyzer, CWE, Ardmore, PA). Immediately prior to initiating recordings, a 1 mg/kg dose of pancuronium (Sandoz, Boucherville, QC) was administered to eliminate muscle tone. The effects of pancuronium were allowed to wear off periodically to confirm a surgical level of anaesthesia, which was monitored by observing pupil diameter and response to a noxious pinch of a forepaw. Supplemental sodium pentobarbital and pancuronium were administered at one-third of the previous dose, approximately each hour via the jugular cannula.

Intracellular recordings from somata in the exposed DRG were made with borosilicate glass micropipettes (1.2 mm outside diameter, 0.68 mm inside diameter; Harvard Apparatus, Holliston, MA). The electrodes were pulled using a Brown-Flaming pipette puller (model P-87; Sutter Instrument Co., Novota, CA). These electrodes were filled with 3 M KCl (DC resistance 50–70 MΩ). Signals were recorded with a Multiclamp 700B amplifier (Molecular Devices, Union City, CA)

and digitized on-line via the Digidata 1322 A interface (Molecular Devices) with pClamp 9.2 software (Molecular Devices). The microelectrode was advanced using an EXFO IW-800 micromanipulator (EXFO, Montreal, QC) in 2 μm steps until an abrupt hyperpolarization of at least 40 mV appeared. Once a stable membrane potential was confirmed, a single stimulus was applied to the dorsal root to provoke an action potential (AP). The protocol editor function in the pClamp 9.2 software was used to evoke a somatic AP by stimulation with a single rectangular intracellular depolarizing voltage pulse.

The first AP evoked by stimulation of the dorsal root and measured at the DRG soma in each neuron was used to compare the configuration between sham and CIP rats. Criteria for inclusion of neurons in the subsequent analysis included a stable resting membrane potential (Vm) more negative than −40 mV, with a somatic spike evoked by dorsal root stimulation of >40 mV. Variables in AP configuration included Vm, AP amplitude (APA), AP duration at base (APdB), AP rise time (APRT), AP fall time (APFT), after-hyperpolarization amplitude (AHPA) and after-hyperpolarization duration to 50% recovery (AHP50). The distance from the stimulation site (cathode) to the recording site (centre of the DRG) was measured at the end of the experiment to determine conduction distance. This value was used to calculate the conduction velocity (CV) of the dorsal root axon associated with each neuron.

Functional classification of DRG neurons. In addition to DRG sensory neuron AP configuration, DRG sensory neurons were classified according to their CV (C-fibre neurons ($\leq$0.8 mm/ms), Aδ-fibre neurons (1.5–6.5 mm/ms) and Aβ-fibre neurons (>6.5 mm/ms)), and receptive properties were defined using hand-held mechanical stimulators as previously described.[30,31] The threshold of activation, the depth of the receptive field and the pattern of adaption were the major factors used to further classify neurons into LTM, HTM and unresponsive neurons. HTM neurons responded to noxious stimuli, including a noxious pinch and application of sharp objects such as the sharp end of a syringe needle, whereas LTM neurons responded to innocuous stimuli such as a moving brush, light pressure with a blunt object, a light manual tap or vibration. Many Aβ-fibre LTM neurons are CUT and include guard/field neurons, rapidly adapting neurons, Pacinian afferents and slowly adapting neurons. A group of neurons with deeper receptive fields that were very sensitive to light pressure and/or leg movement and often showed ongoing activity were classified as MS neurons. These neurons also exhibited slow adaptation to dorsal root stimulation, to intracellular injection of depolarizing current and to leg movement. It should be noted that, as excitability of sensory

neurons can be altered in models of peripheral neuropathy, functional classification was based primarily on responses to the activation of the peripheral receptive fields. However, classification was also based on AP configuration and on responses to activation. Unresponsive and heat neurons were excluded in the present study.

Excitability of DRG neurons

Excitability was measured by evoking APs in DRG neurons using stimulation of the soma by direct injection of depolarizing current.[30] To quantify soma excitability, the threshold of depolarizing current pulses injected into the soma was determined by applying pulses of 100 ms in increments of 0.1 nA through the recording electrode until an AP was evoked or until a maximum current of 4 nA was reached. The excitability of the soma was also evaluated by comparing the number of APs evoked by injecting defined current pulses to the DRG soma; intracellular current injections of 100 ms each were delivered with a 2 nA amplitude.

X-ray radiography and histology

After electrophysiological recordings, the ipsilateral hind limbs of sham and CIP rats were immediately dissected, fixed in a freshly prepared solution of 10% paraformaldehyde in phosphate-buffered saline (PBS) and decalcified in 10% ethylenediaminetetraacetic acid (EDTA). High-resolution radiographic scans of dissected rat femurs were acquired with a Faxitron X-ray MX-20 system (Faxitron, Lincolnshire, IL) on Kodak MIN-R 2000 Mammography Film (Kodak, Rochester, NY). Samples remained in the solution for four weeks, with solution replacement every third day.

Upon completion of decalcification, tissues were dehydrated, embedded in paraffin wax and coronally sectioned at 5 μm. Slide-mounted tissues were heated at 60°C for 1 h prior to haematoxylin and eosin (H&E) staining. Once cool, slides were deparaffinized in three consecutive changes of xylene for 5 min each and rehydrated in increasing concentrations of ethanol. Slides were then immersed in water, followed by immersion in haematoxylin (Gill Number 3, GHS332-1 L; Sigma-Aldrich Canada Ltd), diluted with water to a ratio of 1:2 for 3 min, followed by water, alkaline lithium carbonate for 10 s to change the colour of the haematoxylin stain to blue, water and 45 s in eosin solution (diluted 1:3 in 80% ethanol). Slides were then dehydrated, cleared in xylene, cover-slipped with Permount (SP15-100 Toluene Solution; Fisher Scientific Company, Toronto, ON, Canada) and allowed to dry overnight. H&E tissue staining was then carried out. Other serial coronal sections were immediately immunofluorescently stained to detect cytokeratin 7 (CK7), a marker of epithelial tissue,

to confirm the presence of viable MRMT-1 breast cancer cells within the ipsilateral femurs at endpoint. Slide-mounted tissues were rehydrated, exposed to antigen retrieval in EDTA (pH 8, 95°C) for 20 min, blocked (Dako protein block) for 2 h, incubated in primary (Santa Cruz anti-cytokeratin 7, 1:1000, O/N at 4°C) and fluorescent secondary (Life Technologies AlexaFluor-647 goat anti-mouse, 1:500, 2 h at RT) antibodies, counterstained with DAPI, cover-slipped and imaged using the EVOS FL Cell Imaging System.

In vivo injection of glutamate and SSZ

SSZ (Sigma-Aldrich, St. Louis, MO), an inhibitor of system x_C^-, was prepared in accordance with the manufacturer's recommendations in 1 M NH_4OH. A 1 M stock of the glutamate receptor agonist L-glutamic acid monosodium salt (Sigma-Aldrich) was prepared in PBS (pH 7.4). Both SSZ and L-glutamic acid were then diluted with PBS to final concentrations of 1 mM and 100 mM, respectively, and administered via intramuscular injection at the quadriceps femoris muscle located near the femoral head. SSZ was administered at a dose of 6.6 mg/kg. L-glutamic acid was delivered at 16.9 mg/kg.

Expression of glutamate receptors at the mRNA level in relevant DRG

Glutamate receptor expression at the mRNA level was determined by reverse transcription polymerase chain reaction (RT-PCR) using rat-specific primers. DRG and brain tissue were freshly isolated from sham and CIP rats, immediately flash-frozen in liquid nitrogen and stored at −80°C. Total RNA was extracted with the Qiagen RNeasy Mini Kit according to the manufacturer's protocol and processed with the Ambion DNase Treatment kit prior to spectrophotometric quantification at OD_{260}, with purity verified using OD_{260}/OD_{280}. Reverse transcription was performed using the SuperScript III First-Strand Synthesis System (Invitrogen). PCR with the Abm Taq DNA Polymerase Kit (Invitrogen) was used according to optimized conditions determined for each specific rat primer pair (Table 1). RT-PCR products were run on 2% agarose gels for 1 h at 100 volts to resolve expected bands by size, with specificity being confirmed by bi-sequencing.

Statistical analysis of behavioural and electrophysiological data

In vivo behavioural data were analysed across groups with the Kruskal–Wallis test for non-parametric data with a Dunn's Multiple Comparison post hoc test. Data derived from the in vitro ^{14}C-cystine uptake assay were analysed with a one-way repeated-measures analysis of variance. Electrophysiological data for

Table 1. Rat-specific primers used to detect GluRs in brain and DRG via RT-PCR.

Gene symbol	Primer sequence (5′–3′)	Product size (bp)
NMDA1	F: TCCTATGACAACAAGCGCGG	188
	R: CCAGAGCCCGTCATGTTCAG	
mGluR7	F: TCCACCCTGAACTCAATGTCC	159
	R: CAGCAGGGCTGTTTGGGTCTA	
mGluR8	F: CCAAACATCAACCGCACAGG	153
	R: GGGCGTGTCATTATAGCGGA	

Note: Primers in italic font were detected in the DRG. F corresponds to forward primer, and R to reverse primer. Product sizes are listed in base pairs (bp).

comparing configuration analysis among three groups are presented as the mean ± standard error of the mean (SEM) and were analysed using the Kruskal–Wallis test for non-parametric data with a Dunn's Multiple Comparison post hoc test. Electrophysiological data for comparing pre- and post-treatments are presented as the mean ± SEM and were analysed using the paired t test. $P < 0.05$ was considered to indicate a significant difference. GraphPad Prism software (GraphPad Software, Inc., La Jolla, CA) was used for all statistical analyses and graphing.

Results

Comparison between CIP-W2 and CIP-W3 rats

Comparison of nociceptive behaviour and bone tumours. A behavioural test of tactile hypersensitivity was based on changes in paw withdrawal thresholds from von Frey filaments. Baseline levels established for the Von Frey behavioural test were 13.35 ± 1.02 g, and rats were then randomly assigned into control (sham) as well as two CIP groups. Von Frey tests, performed again immediately prior to electrophysiological experiments, revealed decreased mechanical withdrawal thresholds for limbs bearing tumour relative to thresholds obtained from sham-implanted (control) rats (Figure 1). Withdrawal thresholds were 13.99 ± 1.98 g in the control group, 5.59 ± 4.90 g in the CIP-W2 group and 4.06 ± 2.94 g in the CIP-W3 group. Differences between the three groups were significant ($P = 0.003$) as determined using the Kruskal–Wallis test, with $P < 0.05$ between the control versus CIP-W2 and control versus CIP-W3 groups, while no significant difference between CIP-W2 and CIP-W3 groups was obtained using the Dunn's Multiple Comparison post hoc test.

H&E-stained sections of the ipsilateral distal femur sections from CIP rats indicated tumour replacement of marrow. Immunohistochemical and immunofluorescent staining of tumour-bearing limbs demonstrated the
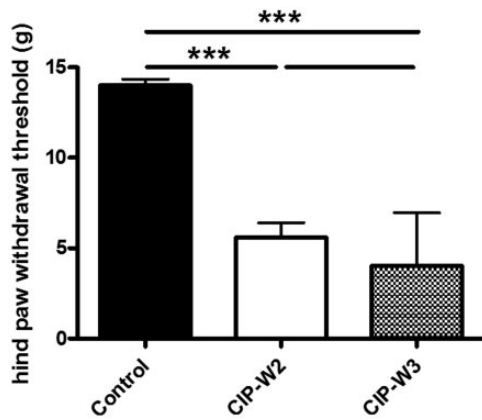
Figure 1. Comparison of the 50% withdrawal thresholds between control (sham) and CIP rats. Withdrawal thresholds to mechanical stimulation of the plantar surface of the tumour-bearing hind paw with von Frey filaments were recorded on the same day immediately before acute electrophysiological experiments. CIP-W2: 14–16 days post-model induction; CIP-W3: 21–28 days post-model induction; Control: sham-injected (n = 6 for each group). Asterisks above the graph indicate a significant difference between the indicated groups, with ***$P < 0.001$ determined by the Kruskal–Wallis test for non-parametric data with a Dunn's multiple comparison post hoc test. CIP: cancer-induced pain.

presence of carcinoma cells ex vivo (Figure 2), confirming the presence of MRMT-1 cells at endpoint in CIP-implanted rats. The main difference between the CIP-W2 and CIP-W3 groups was that the tumours were conserved within the epiphysis, eroding trabecular bone in CIP-W2 rats (Figure 2(a) to (c)). Evidence supporting osteolytic degradation was also visible in radiographs of tumour-bearing hind limbs (Figure 2(d) and (e)). In CIP-W3 rats, clear osteolytic degradation was observed, which could not be confirmed in CIP-W2 rats.

Comparison of AP configurations of DRG neurons. The following parameters were analysed from intracellular recordings of somatic APs evoked by electrical stimulation of the dorsal root: (1) CV, (2) Vm, (3) APA, (4) APdB, (5) APRT, (6) APFT, (7) AHPA and (8) AHP50. Intrasomal recordings were made from a total of 124 L4 DRG neurons in three groups (six rats in each group). All neurons met the inclusion criteria described in the methods section for HTM and LTM (CUT and MS) neurons. Table 2 shows the mean value for each group, the corresponding standard error of the mean, and the *P* value for comparisons among groups. There were no significant differences in CV, Vm, AHPA and
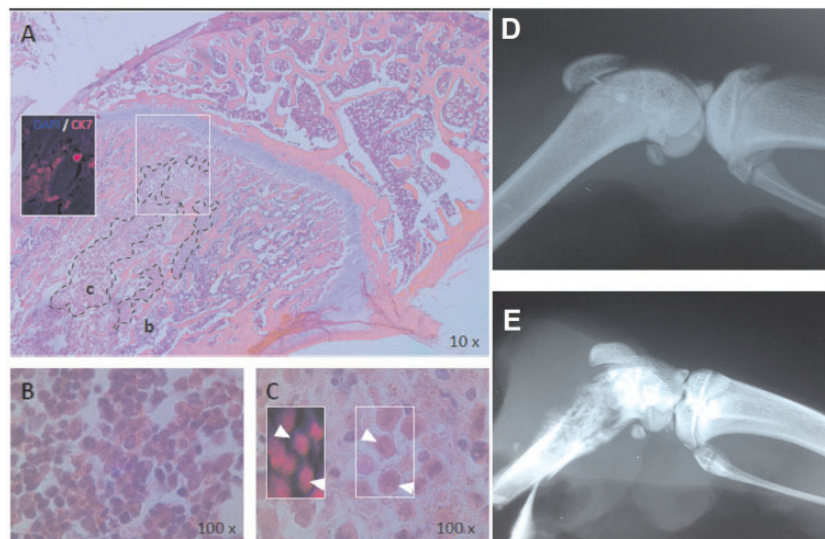

Figure 2. Comparison of haematoxylin and eosin-staining and X-ray imaging of tumour-bearing femurs between control (sham) and CIP rats. (a) Haematoxylin and eosin-stained tissue in a representative CIP-W2 rat. Serially sectioned immunofluorescence demonstrated specific staining with cytokeratin 7 (CK7), a marker of epithelial tissue, confirming the presence of MRMT-1 breast cancer cells within tumour-bearing femurs. Brightfield and corresponding fluorescent images (10×) of MRMT-1-inoculated femurs at endpoint. Dash-enclosed areas indicate the tumour cell mass, with the insert depicting CK7-positive cells (pink) within the bone microenvironment. Letters correspond to magnified photomicrographs of (b) bone not infiltrated by MRMT-1 cells and (c) bone bearing the tumour. (b and c) Magnified photomicrographs (100×) of areas representing (b) non-tumour bearing bone and (c) tumour-bearing bone. Arrows indicate MRMT-1 cells. Areas normally containing uncompromised bone tissue have been replaced with MRMT-1 cells. (d and e) Evidence of osteolytic degradation was also visible in radiographs of cancer cell-injected ipsilateral hind legs of (d) CIP-W2 and (e) CIP-W3 rats, with CIP-W3 rats showing clear osteolytic degradation.

Table 2. Comparison of the action potential configuration of DRG neurons between control (sham) and CIP rats.

Class of neuron	Number of neurons per group	CV (mm/ms)	Vm (−mV)	APA (mV)	APdB (s)	APRT (s)	APFT (s)	AHPA (mV)	AHP50 (s)
CHTM	Control (n = 11)	0.56 ± 0.101	67.23 ± 8.673	83.16 ± 9.094	3.20 ± 0.549	1.45 ± 0.267	1.75 ± 0.515	9.06 ± 3.125	12.83 ± 9.692
	CIP-W2 (n = 10)	0.53 ± 0.137	58.37 ± 8.680	65.24 ± 13.11	2.23 ± 0.773	1.14 ± 0.166	1.10 ± 0.742	6.51 ± 4.738	6.29 ± 6.676
	CIP-W3 (n = 10)	0.57 ± 0.118	57.2 ± 9.096	70.89 ± 7.111	2.47 ± 0.538	1.14 ± 0.229	1.33 ± 0.587	8.85 ± 2.507	10.4 ± 4.031
	P	0.795	**0.033**	**0.003**	**0.009**	**0.005**	0.091	0.303	0.056
AβHTM	Control (n = 10)	12.69 ± 2.168	64.22 ± 9.071	81.06 ± 8.851	1.71 ± 0.175	0.64 ± 0.070	1.07 ± 0.129	7.88 ± 3.378	11.77 ± 10.4
	CIP-W2 (n = 10)	11.23 ± 3.337	60.17 ± 9.366	60.17 ± 9.366	1.72 ± 0.512	0.72 ± 0.268	1.00 ± 0.317	6.57 ± 4.151	5.36 ± 5.545
	CIP-W3 (n = 10)	13.81 ± 3.286	67.94 ± 9.287	67.94 ± 9.287	1.74 ± 0.196	0.72 ± 0.103	1.03 ± 0.153	10.45 ± 2.925	9.80 ± 6.882
	P	0.211	0.134	**0.015**	0.422	0.304	0.184	0.083	0.147
MS	Control (n = 21)	17.54 ± 4.171	63.34 ± 9.998	60.37 ± 6.678	0.87 ± 0.187	0.42 ± 0.099	0.45 ± 0.252	6.15 ± 3.573	1.61 ± 0.792
	CIP-W2 (n = 19)	17.90 ± 4.876	64.58 ± 9.967	54.17 ± 4.857	1.11 ± 0.247	0.52 ± 0.1	0.59 ± 0.305	7.87 ± 4.774	1.95 ± 0.665
	CIP-W3 (n = 19)	18.90 ± 2.672	64.53 ± 5.371	56.88 ± 11.96	1.11 ± 0.249	0.51 ± 0.081	0.60 ± 0.265	5.96 ± 4.454	2.11 ± 0.941
	P	0.312	0.798	**0.009**	**0.007**	**0.005**	0.263	0.511	0.114
CUT	Control (n = 23)	16.05 ± 3.095	67.18 ± 7.946	64.47 ± 11.030	1.24 ± 0.201	0.50 ± 0.099	0.73 ± 0.257	8.26 ± 5.257	5.84 ± 4.800
	CIP-W2 (n = 21)	14.72 ± 3.450	66.32 ± 9.822	57.24 ± 6.323	1.56 ± 0.405	0.61 ± 0.161	0.95 ± 0.288	5.44 ± 3.795	5.95 ± 6.417
	CIP-W3 (n = 21)	15.20 ± 3.328	64.55 ± 7.763	57.91 ± 9.127	1.52 ± 0.401	0.61 ± 0.148	0.91 ± 0.439	5.92 ± 4.179	4.02 ± 3.357
	P	0.482	0.554	**0.036**	**0.003**	**0.008**	0.051	0.111	0.292

Note: Statistical tests for each variable were carried out on sensory neuron subgroups comparing control and CIP rats. The mean ± SEM of measured variables are listed. The p value is shown below each section, indicating the level of significance, with $P < 0.05$ indicated in bold. n: the number of neurons in each group; CV: conduction velocity; Vm: resting membrane potential; APA: action potential amplitude; APdB: action potential duration at base; APRT: action potential rise time; APFT: action potential fall time; MRR: maximum rising rate; MFR: maximum falling rate; AHPA: after-hyperpolarization amplitude; AHP50: after-hyperpolarization duration at 50% recovery; CHTM: C-fibre high-threshold mechanoreceptive neurons; CUT: cutaneous neurons; MS: muscle spindle neurons.
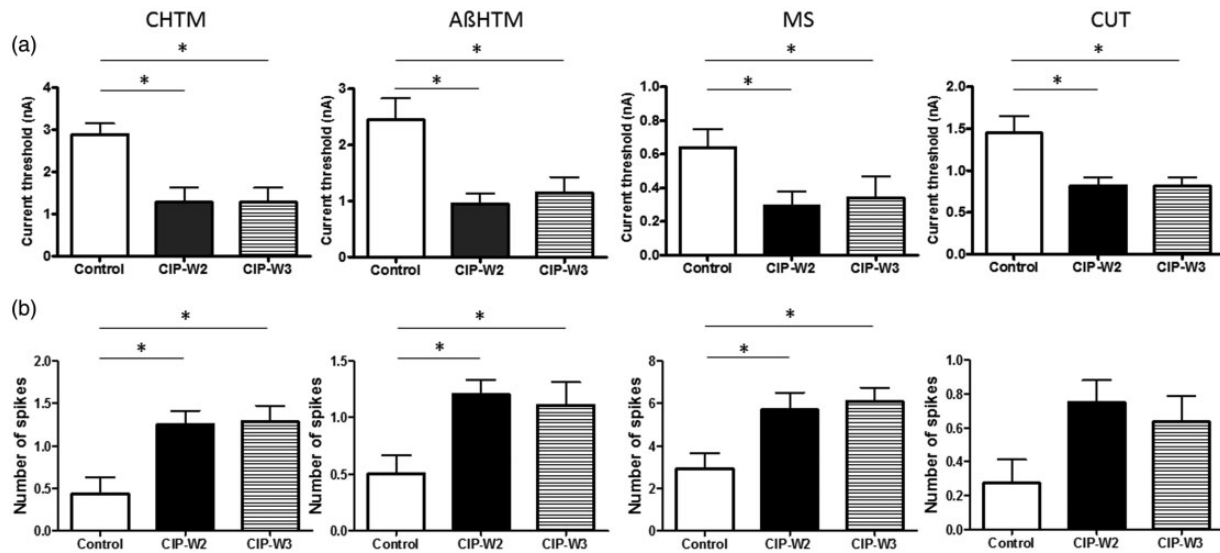
Figure 3. Comparison of the activation of DRG sensory neurons in response to intracellular current injection between control (sham) and CIP rats. (a) The current threshold was defined as the minimum current required to evoke an AP by intracellular current injection. Excitability of the DRG soma was significantly increased in CIP rats, as indicated by a decreased activation threshold in both CIP-W2 and CIP-W3 neurons. (b) Comparison of the repetitive discharge characteristics of DRG produced by intracellular current injection. Bar graphs show the number of APs evoked by intracellular depolarizing current injection of 2 nA, 100 ms. Asterisks above the graphs indicate a significant difference between control and CIP-W2 and CIP-W3 animals. *$P < 0.05$ was obtained using a Kruskal–Wallis test for non-parametric data with a Dunn's multiple comparison post hoc test. CHTM: C-fibre high-threshold mechanoreceptor; MS: muscle spindle neuron; CUT: cutaneous neuron; CIP: cancer-induced pain.

AHP50 between groups for all comparisons. The APA of CHTM, AβHTM and MS neurons; the APdB of CHTM, MS and CUT neurons; and the APRS of CHTM neurons showed significant difference among groups ($P < 0.05$). Post hoc comparisons showed that these parameters in the control group were significantly different compared to the CIP-W2 and CIP-W3 groups ($P < 0.05$), which did not differ from one another.

Comparison of the excitability of the soma measured by responses to injection of depolarizing current. AP responses to intracellular depolarizing current injection were recorded to determine whether there were differences in soma excitability in the CIP-W2 and CIP-W3 groups relative to the sham control group. Figure 3(a) illustrates the threshold currents that elicited APs in each of the three groups. CHTM (Control: 2.89 ± 0.71 (n = 7), CIP-W2: 1.29 ± 0.91 (n = 8), CIP-W3: 1.29 ± 0.91 (n = 7)); AβHTM (Control: 2.44 ± 1.16 (n = 10), CIP-W2: 0.95 ± 0.60 (n = 10), CIP-W3: 1.15 ± 0.88 (n = 9)); MS (Control: 0.64 ± 0.35 (n = 10), CIP-W2: 0.29 ± 0.26 (n = 10), CIP-W3: 0.34 ± 0.41 (n = 10)); and CUT (Control: 1.45 ± 0.70 (n = 11), CIP-W2: 0.82 ± 0.33 (n = 12), CIP-W3: 0.82 ± 0.34 (n = 11)) neurons showed significant differences among the three groups ($P < 0.05$). Post hoc comparisons revealed a significant decrease in the threshold necessary to elicit a response in CIP-W2 and CIP-W3 rats relative to controls ($P < 0.05$),

with no significant differences between the CIP-W2 and CIP-W3 groups.

Figure 3(b) shows the number of APs elicited in response to a 2 nA current injection. With the exception of CUT neurons (Control: 0.27 ± 0.47 (n = 11), CIP-W2: 0.75 ± 0.45 (n = 12), CIP-W3: $0.64 \pm 0. 51$ (n = 11)); CHTM (Control: 0.43 ± 0.54 (n = 7), CIP-W2: 1.25 ± 0.46 (n = 8), CIP-W3: 1.29 ± 0.49 (n = 7)); AβHTM (Control: 0.50 ± 0.53 (n = 10), CIP-W2: 1.20 ± 0.42 (n = 10), CIP-W3: 1.11 ± 0.60 (n = 9)); and MS (Control: 2.90 ± 2.38 (n = 10), CIP-W2: 5.7 ± 2.54 (n = 10), CIP-W3: 6.10 ± 2.03 (n = 10)) neurons showed significant difference among the three groups ($P < 0.05$). Post hoc comparisons revealed significantly increased numbers of elicited APs in response to a 2 nA stimulation in CIP-W2 and CIP-W3 rats relative to controls ($P < 0.05$), whereas no significant differences between CIP-W2 and CIP-W3 groups were obtained.

Inhibition of system x_C^- activity by SSZ in vitro

SSZ, a known inhibitor of system x_C^-, dose-dependently blocked the activity of this antiporter in MRMT-1 breast carcinoma cells over a range of 0–1000 μM when applied to these cells in vitro (Figure 4). SSZ caused a robust decrease in cystine uptake at the 1000 μM dose within 5 min ($P < 0.05$; Figure 4(a)), with a peak effect at 15 min ($P < 0.05$; Figure 4(b)) as determined in a 30-min time
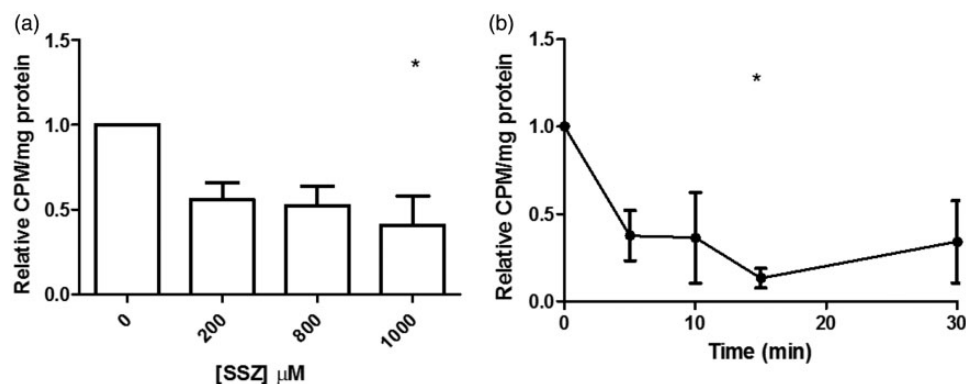
Figure 4. In vitro inhibition of system x_C^- activity by SSZ in MRMT-1 cells. (a) ^{14}C-cystine uptake in MRMT-1 breast carcinoma cells following a 5-min incubation with SSZ. Cells were seeded at 1×10^5–2.5×10^5 cells per well, and after 24 h, these were treated with SSZ in HBSS at concentrations ranging from 0 to 1000 μM. (b) ^{14}C-cystine uptake in MRMT-1 breast carcinoma cells incubated with 1000 μM of SSZ over a 30-min time course. Data represent the mean of n = 3 experiments ± SEM, and significance was determined to be *$P < 0.05$ by one-way repeated-measures analysis of variance. SSZ: sulphasalazine.

course experiment. Drug vehicle control (DMSO) did not alter system x_C^- activity (0 μM).

Sensory neuron excitability is altered in response to changes in peripheral glutamate

Changes in soma excitability profiles in response to SSZ injection in CIP rats. To determine whether peripherally administered SSZ affects the excitability of DRG soma of tumour-bearing animals in vivo, this agent was intramuscularly injected near the femoral head of CIP rats. The responses of CHTM (n = 5), AβHTM (n = 4), MS (n = 4) and CUT (n = 4) neurons decreases within 5 min post-SSZ injection, as evaluated by their respective changes in soma excitability (Figure 5(a)). Two of above neurons in each neuronal catalogue were successfully traced over a 30-min course, with recordings obtained at 5, 10, 15 and 30 min. A comparison of the excitability pre- and post-injection over the entire 30-min recording time frame in each neuronal catalogue is shown in Figure 5(b). One CHTM neuron stopped spiking within 30 min, while the second of this class increased its threshold within 30 min. One AβHTM neuron increased its threshold and resumed activity at 30 min, while the other stopped spiking within 30 min. One MS sensory neuron increased its threshold and resumed at 30 min with decreasing numbers of spiking, and the other MS sensory neuron did not change its threshold but decreased the number of spiking during 30-min time course. One CUT sensory neuron increased its threshold and resumed at 15 min, and the other CUT sensory neuron increased its threshold within the 30 min time course. Figure 5(c) shows one representative discharge pattern of soma changes in response to peripheral SSZ injection within the 30 min time course for each type of neuron.

Changes in soma excitability profiles in response glutamate injection in sham animals. In contrast to results obtained with peripheral SSZ injection, when L-glutamic acid was injected into sham rats (n = 8), excitability of the soma in CHTM (n = 5), AβHTM (n = 4), MS (n = 4) and CUT (n = 4) neurons was dramatically increased in 5 min (Figure 6(a)). A comparison of the excitability between pre- and post-L-glutamic acid injection over the entire 30-min recording time frame in each neuronal catalogue (n = 2 each from above neurons) is shown in Figure 6(b). One CHTM neuron decreased its threshold at 5 min and returned to the original state by 15 min, and the threshold of the second CHTM decreased within 30 min of the time course. One AβHTM exhibited a decreased threshold with an increased number of spiking at 5 min, resuming at 30 min, and the other neuron had a decreased threshold within 30 min. Both MS sensory neurons did not exhibit a change in their threshold but showed cycled increases, returning to the number of spikes within the 30-min time course. One CUT sensory neuron decreased the threshold and resumed at 15 min and the other CUT neuron decreased the threshold within 30 min. Figure 6 (c) illustrates typical discharge patterns of soma evoked in response to glutamate injection over the 30-min time course. Neuronal excitability increased within 5 min, returning to the original state by 15–30 min or longer (30 min is the cut-off time). One AβHTM neurons was auto-spiking within 5 min after glutamate injection (Figure 6(d)).

Expression of glutamate receptors at the mRNA level in relevant DRG. The presence of ionotropic and metabotropic GluR subunits was assessed at the mRNA levels in DRG obtained from CIP and control rats. Brain tissue was used as a positive control, with water only serving as a negative control to demonstrate that the resulting
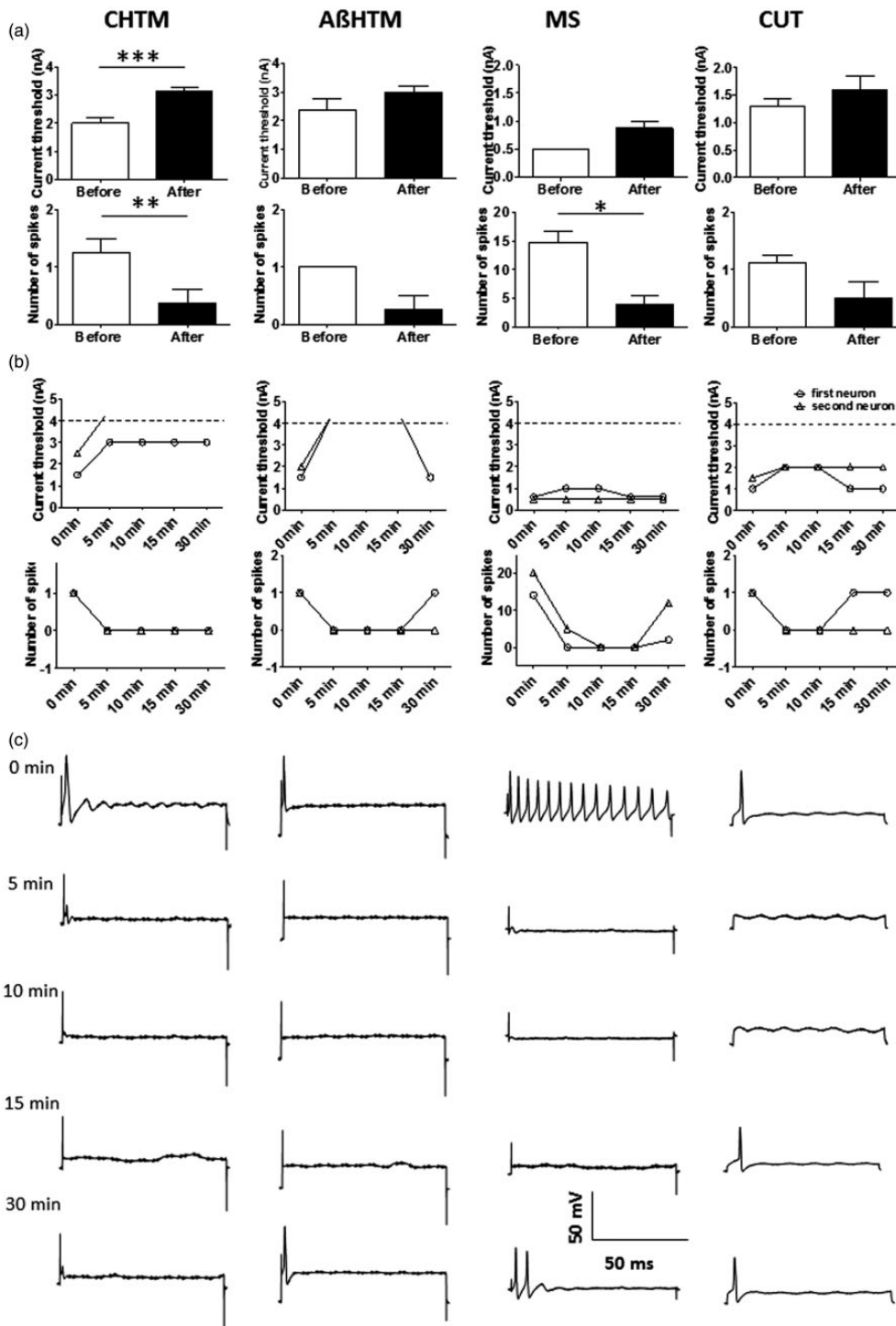
Figure 5. Excitability changes of DRG sensory neurons in CIP-W2 rats in response to peripheral SSZ injection. (a) Comparison of the threshold and number of spikes of each class of sensory neurons pre- and post-injection at 5 min. The upper panel illustrates a comparison of threshold currents of the sensory neurons that elicited APs pre- and post-SSZ injection. The lower panel depicts a comparison of the number of APs that were elicited pre- and post-SSZ injection by intracellular depolarizing current stimulation of 2 nA, 100 ms. Data represent the mean ± SEM, and significance was determined to be *$P<0.05$, **$P<0.01$ and ***$P<0.001$ by paired t test. (b) Comparison of the threshold (upper panel) and number of spikes at threshold (lower panel) pre- and post-injection during a 30-min time course. Profiles for two individual neurons in each neuronal class are shown at 5, 10, 15 and 30 min. In some cases, no spiking after treatment occurred upon reaching the 4 nA maximum threshold. (c) Representative raw recordings (for one of the two neurons recorded in (b)) exhibited discharge characteristics of DRG sensory neurons within the 30-min time course. The following current injection pulses which initially evoked an action potential prior to treatment were chosen for tracing individual neurons: CHTM (100 ms, 1.50 nA); AßHTM (100 ms, 1.5 nA); MS (100 ms, 0.5 nA); CUT (100 ms, 1 nA). CHTM: C-fibre high-threshold mechanoreceptor; MS: muscle spindle neuron; CUT: cutaneous neuron.
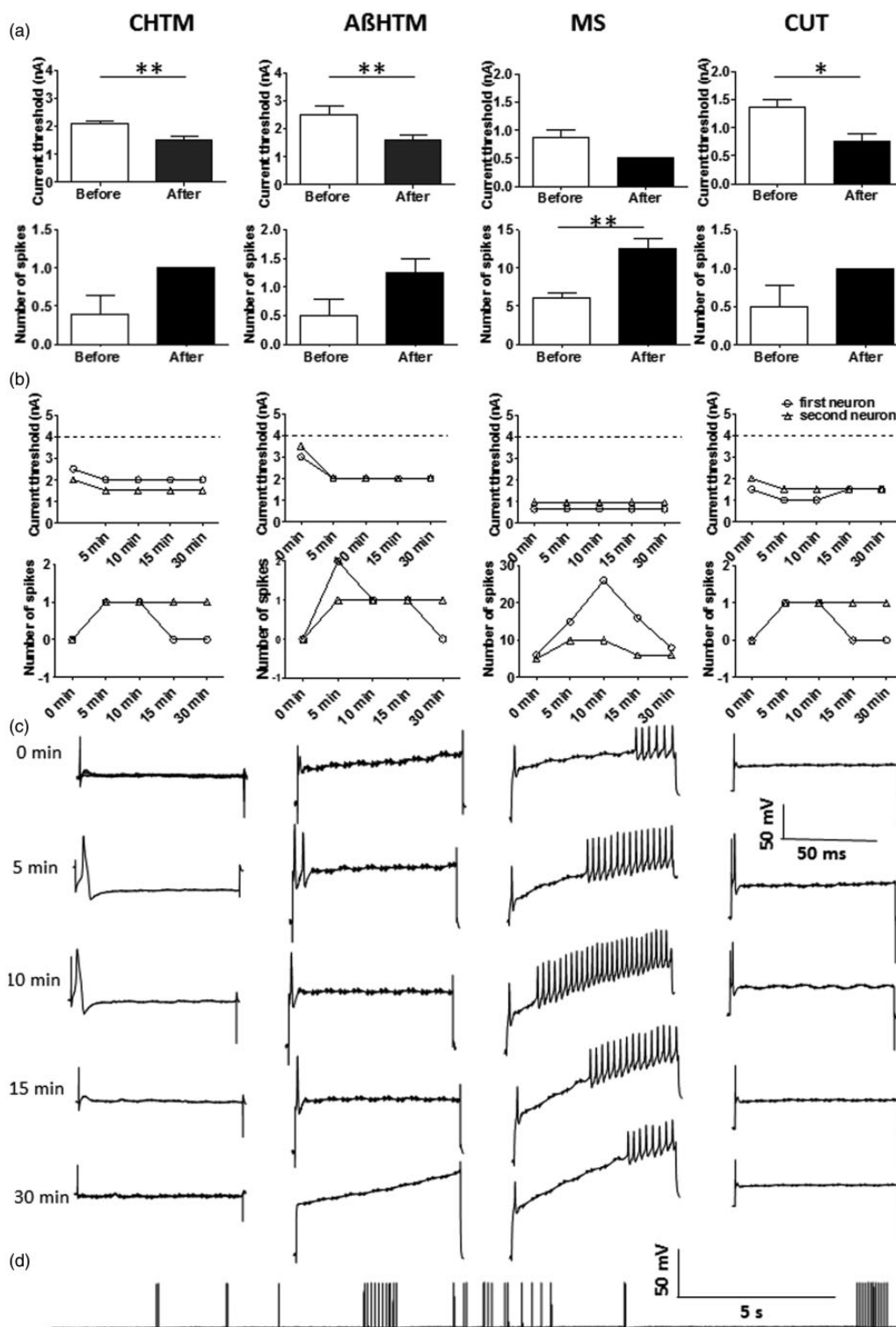
Figure 6. (a) Comparison of the threshold and number of spikes of each class of sensory neurons pre- and post-injection at 5 min. The upper panel illustrates a comparison of threshold currents of the sensory neurons that elicited APs pre- and post-glutamate injection. The lower panel depicts a comparison of the number of APs elicited pre- and post-glutamate injection by intracellular depolarizing current stimulation of 2 nA, 100 ms. Data represent the mean ± SEM, and significance was determined to be *P<0.05 and **P<0.01 by paired t test. (b) Comparison of the threshold (upper panel) and the number of spiking at threshold (lower panel) of sensory neurons pre- and post-glumate injection. Data were obtained from two representative neurons in each neuronal class from naïve rats. (c) Representative raw recordings (for one of the neurons in (b)) exhibited discharge characteristics of DRG sensory neurons within the 30-min time course. The following current injection pulses which initial evoked action potential prior to treatment were chosen for tracing individual neurons: CHTM (100 ms, 2 nA); AßHTM (100 ms, 2 nA); MS (100 ms, 0.5 nA); CUT (100 ms, 1 nA). (d) A raw recording of AßHTM auto-discharge 5 min after glutamate injection. CHTM: C-fibre high-threshold mechanoreceptor; MS: muscle spindle neuron; CUT: cutaneous neuron.
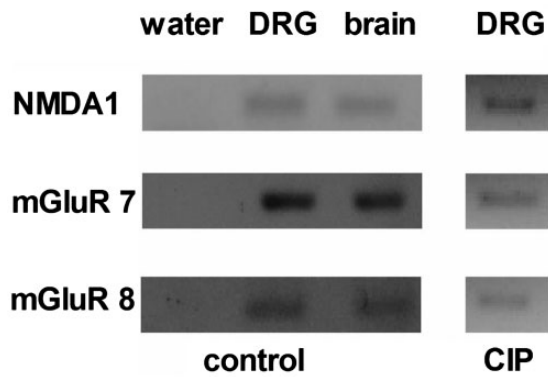
Figure 7. Ionotropic and metabotropic glutamate receptor sub-unit mRNA is present in DRG isolated from control (sham) and CIP rats. Representative RT-PCR products for NMDA1, mGluR7 and mGluR8, with brain tissue used as a positive control and water used as negative control to confirm the absence of contaminants. Expected sizes in base pairs (bp) are indicated for each RT-PCR product. CIP: cancer-induced pain; DRG: dorsal root ganglia.

bands were not due to contaminants in the RT-PCR reaction. Of a list of representative GluRs, NMDA1, mGluR7 and mGluR8 were detected in both CIP- and sham-injected rats. Representative RT-PCR products are shown in Figure 7.

Discussion

We previously showed in a rat CIP model that not only HTM but also LTM (CUT and MS) neurons showed plastic activity in DRG.[5,6] We also reported that changes in intrinsic membrane properties and excitability of normally non-nociceptive Aβ sensory neurons occur in the rat CIP model as well as a rat model of peripheral neuropathic pain induced by a sciatic nerve cuff.[32] To answer the question whether a bone tumour initiated from metastatic breast carcinoma cells affects the processes of sensory neurons, we separated the CIP model into two groups: one in which tumours were confined within the bone (CIP-W2) and another in which tumours initiated in the femur were allowed to grow out of the bone, an event that occurs at later stages post-cancer cell injection (CIP-W3). We found that all mechanoreceptor neurons showed similar plastic activity in DRG in both models, suggesting that tumours restricted to bone, as well as bone tumours that spread to affect the surrounding tissue as they continue to grow, induce systemic neurochemical changes. These changes may not only induce skeletal dysfunctions and accompanying bone pain but may also evoke muscular dysfunction accompanied by CUT pain.

In our previous study based on an immunocompromised mouse model of CIP, we established that blocking system x_C^--mediated glutamate release from human breast cancer cells using SSZ delays the onset of

nociceptive behaviours,[10] indicating that glutamate derived from a bone tumour may play an important role in generating or perpetuating this type of pain. Furthermore, we have previously shown that implanting human breast cancer cells in which *xCT*, the functional component of system x_C^-, was specifically knocked down into a immunocompromised mouse CIP model supports this notion.[11] In the current investigation, we confirmed via time course analysis that SSZ rapidly inhibits glutamate release from rat MRMT-1 cells in vitro. Based on these results, a dose of SSZ was selected for in vivo application in the rat CIP model, which was adapted to assess nociceptive intracellular electrophysiological characteristics. Here, we clearly demonstrated the inhibitory effect of SSZ on the activity of peripheral sensory neurons assessed at the level of the DRG in animals with CIP, in conjunction with the opposing excitatory effect elicited by glutamate injection into sham animals. These results strongly support that the sensitizing effect of local bone tumour-produced glutamate is mediated through the activation of peripheral sensory neurons. The findings reported in the current investigation differ from the SSZ-mediated effect on nociceptive behaviours that we showed in our previous work, in which this agent was delivered chronically via an intraperitoneal pump, rather than being acutely delivered via intramuscular injection at the femoral head to examine real-time changes in peripheral nerve impulses.

It could be argued that the effect of glutamate on peripheral sensory neurons may be due to descending pain pathway modulation and facilitation. However, the L4 dorsal root assessed in our study was transected close to the spinal cord, and uptake glutamate from the peripheral circulation was therefore limited by the blood–brain barrier to most central regions.[28] Therefore, changes in the excitability of sensory neurons integrated within the L4 DRG in response to glutamate are likely to be a response of the PNS.

Guedon et al. presented several possible mechanisms that could drive bone cancer-induced CUT hypersensitivity,[1] including DRG dysfunction,[33,34] spinal sensitization[35,36] and central sensitization.[2,37,38] All three mechanisms could result in altered descending modulation and ascending facilitation of noxious and non-noxious sensory input.[1] In our study, injection of L-glutamic acid or SSZ into the quadriceps femoris muscle changed the mechanical threshold and spiking number of HTM and LTM sensory neurons within the first 5 minutes. The association of increased glutamate levels with both ongoing nociception and mechanical pain thresholds is consistent with results from previous studies. Although the majority of these studies have reported that elevated levels of glutamate activate the PNS on unmyelinated small diameter sensory neurons (C and Aδ), the effects of glutamate on myelinated

large diameter (Aß) sensory neurons have also been reported. For example, systemic administration of monosodium glutamate (MSG) elevates intramuscular glutamate levels and sensitizes rat masseter muscle afferent fibres.[39] Injection of a relevant dose of MSG into the masseter muscle decreases the mechanical threshold of slowly conducting masseter afferent fibres by as much as 50% within the first 5 minutes post-injection,[39] an effect that is sustained for 3 hours or longer.[23]

As an excitatory neurotransmitter, glutamate is present in vesicular form in the membranes of spinal neurons post-synaptic to nociceptive afferents in order to mediate the activation of glutamate receptors within the CNS. However, anatomical, immunohistochemical and pharmacological studies have provided evidence that both ionotropic and metabotropic glutamate receptors are also expressed by a subpopulation of peripheral unmyelinated and myelinated sensory nerve endings in the skin,[13,40–44] joints[12,20] and the masseter muscle.[23,45,46] The localization of ionotropic receptors, including NMDA receptor subunits (NR1 as well as NRgbs, the glutamate binding subunits of an NMDA receptor complex), several α-amino-3-hydroxy-5-methyl-4-isoxazolepropionic acid (AMPA) receptor subunits (GluR1-4) and a kainate (KA) receptor subunit (GluR5) have been examined in the rat DRG using immunohistochemistry and *in situ* hybridization histochemistry.[47] The authors reported that small neurons (C and Aδ) expressed GluR1- and GluR2/3-like immunoreactivity and GluR5, NR1, NRgbs mRNAs, while large neurons (Aß) expressed GluR2/3-like immunoreactivity and NR1 and NRgbs mRNAs. In the present study, we investigated the expression of ionotropic and metabotropic glutamate receptors in relevant DRG. We demonstrate that NMDA1, as well as mGluR7 and mGluR8, are expressed at the mRNA level in both sham and CIP rats. It is possible that these GluRs are then translated in the soma and transported along axons extending centrally and peripherally.[48] While we have not carried out a quantitative analysis, it has been reported that the proportion of unmyelinated and myelinated axons labelled for NMDA, AMPA and KA receptors in CUT nerves in the paw are significantly increased in an inflammatory model of pain.[41] Although it has been reported that overexpression of metabotropic GluRs such as mGluR2 in DRG induces analgesia in models of inflammatory and neuropathic pain,[49,50] the specific contributions of mGluR7 and mGluR8 with regard to nociception have not been reported.[51] It is possible that CIP induces a reorganization of glutamate receptors on sensory neurons, and that increases in the number of sensory axons containing ionotropic glutamate receptors may contribute to peripheral sensitization. A quantitative analysis of GluR expression needs to be carried out, accompanied by a systematic examination of other glutamate receptor types.

Conclusion

We report here that sensory neurons exhibit similarly increased excitability in a CIP model in which the tumour remains isolated within bone and in a CIP model in which the tumour has extended into the surrounding soft tissue. The activity of these sensory neurons can be inhibited with SSZ upon its local injection into the quadriceps femoris muscle. In addition, these neurons demonstrate excitation in response to intramuscular glutamate injection near the femoral head in sham rats. Therefore, our findings suggest that glutamate released from cancer cells that give rise to a bone tumour excites and induces skeletal and CUT hyperalgesia and mechanical sensitization by potentially activating peripherally expressed GluRs. Our findings add to the growing body of evidence that glutamatergic signalling is involved in generating CIP, contributing to peripheral sensitization and tumour-induced tactile hypersensitivity.

Author Contributions

YFZ designed the experiment, performed all in vivo electrophysiological recordings, analysed the data and prepared the first draft of the manuscript. KL-M critically reviewed and prepared the final version of the manuscript. JW, under the supervision of KL-M, carried out the GluR expression experiment. YFZ and TM carried out the histology experiment. JF performed the in vitro cystine uptake assays. JF and RU cultured the MRMT-1 cells and carried out bone injections to induce CIP. KLZ performed Von Frey tests. All authors contributed to successive drafts of the manuscript and the discussion. GS supervised the overall project, edited the manuscript and provided funding for the study. All authors have read and approved the final manuscript.

ORCID iDs

Katja Linher-Melville ![iD] https://orcid.org/0000-0001-8243-0212
Tanya Miladinovic ![iD] https://orcid.org/0000-0002-4129-7950

References

1. Guedon J-M, Longo G, Majuta LA, Thomspon ML, Fealk MN, Mantyh PW. Dissociation between the relief of skeletal pain behaviors and skin hypersensitivity in a model of bone cancer pain. *Pain* 2016; 157: 1239–1247.
2. Guan X, Fu Q, Xiong B, Song Z, Shu B, Bu H, Xu B, Manyande A, Cao F, Tian Y. Activation of PI3Kγ/Akt pathway mediates bone cancer pain in rats. *J Neurochem* 2015; 134: 590–600.
3. Hald A, Hansen RR, Thomsen MW, Ding M, Croucher PI, Gallagher O, Ebetino FH, Kassem M, Heegaard A-M. Cancer-induced bone loss and associated pain-related behavior is reduced by risedronate but not its phosphono-carboxylate analog NE-10790. *Int J Cancer* 2009; 125: 1177–1185.
4. Honore P, Mantyh PW. Bone cancer pain: from mechanism to model to therapy. *Pain Med Malden Med* 2000; 1: 303–309.
5. Zhu YF, Ungard R, Seidlitz E, Zacal N, Huizinga J, Henry JL, Singh G. Differences in electrophysiological properties of functionally identified nociceptive sensory neurons in an animal model of cancer-induced bone pain. *Mol Pain* 2016; 12: 174480691662877.
6. Zhu YF, Ungard R, Zacal N, Huizinga JD, Henry JL, Singh G. Rat model of cancer-induced bone pain: changes in nonnociceptive sensory neurons in vivo. *Pain Rep* 2017; 2: e603.
7. Seidlitz EP, Sharma MK, Saikali Z, Ghert M, Singh G. Cancer cell lines release glutamate into the extracellular environment. *Clin Exp Metastasis* 2009; 26: 781–787.
8. Bannai S. Exchange of cystine and glutamate across plasma membrane of human fibroblasts. *J Biol Chem* 1986; 261: 2256–2263.
9. Miladinovic T, Nashed MG, Singh G. Overview of glutamatergic dysregulation in central pathologies. *Biomolecules* 2015; 5: 3112–3141.
10. Ungard RG, Seidlitz EP, Singh G. Inhibition of breast cancer-cell glutamate release with sulfasalazine limits cancer-induced bone pain. *Pain* 2014; 155: 28–36.
11. Ungard RG, Linher-Melville K, Nashed M, Sharma M, Wen J, Singh G. xCT knockdown in human breast cancer cells delays onset of cancer-induced bone pain. *Mol Pain* 2019; 15: 1744806918822185.
12. Cairns BE, Hu JW, Arendt-Nielsen L, Sessle BJ, Svensson P. Sex-related differences in human pain and rat afferent discharge evoked by injection of glutamate into the masseter muscle. *J Neurophysiol* 2001; 86: 782–791.
13. Carlton SM. Peripheral excitatory amino acids. *Curr Opin Pharmacol* 2001; 1: 52–56.
14. Beirith A, Santos ARS, Calixto JB. Mechanisms underlying the nociception and paw oedema caused by injection of glutamate into the mouse paw. *Brain Res* 2002; 924: 219–228.
15. Gazerani P, Wang K, Cairns BE, Svensson P, Arendt-Nielsen L. Effects of subcutaneous administration of glutamate on pain, sensitization and vasomotor responses in healthy men and women. *Pain* 2006; 124: 338–348.
16. Jackson DL, Graff CB, Richardson JD, Hargreaves KM. Glutamate participates in the peripheral modulation of thermal hyperalgesia in rats. *Eur J Pharmacol* 1995; 284: 321–325.
17. Carlton SM, Zhou S, Coggeshall RE. Evidence for the interaction of glutamate and NK1 receptors in the periphery. *Brain Res* 1998; 790: 160–169.
18. Zhou S, Bonasera L, Carlton SM. Peripheral administration of NMDA, AMPA or KA results in pain behaviors in rats. *Neuroreport* 1996; 7: 895–900.
19. Davidson EM, Coggeshall RE, Carlton SM. Peripheral NMDA and non-NMDA glutamate receptors contribute to nociceptive behaviors in the rat formalin test. *Neuroreport* 1997; 8: 941–946.
20. Lawand NB, Willis WD, Westlund KN. Excitatory amino acid receptor involvement in peripheral nociceptive transmission in rats. *Eur J Pharmacol* 1997; 324: 169–177.
21. Leem JW, Hwang JH, Hwang SJ, Park H, Kim MK, Choi Y. The role of peripheral N-methyl-D-aspartate receptors in Freund's complete adjuvant induced mechanical hyperalgesia in rats. *Neurosci Lett* 2001; 297: 155–158.
22. Ahn DK, Jung CY, Lee HJ, Choi HS, Ju JS, Bae YC. Peripheral glutamate receptors participate in interleukin-1beta-induced mechanical allodynia in the orofacial area of rats. *Neurosci Lett* 2004; 357: 203–206.
23. Cairns BE, Gambarota G, Svensson P, Arendt-Nielsen L, Berde CB. Glutamate-induced sensitization of rat masseter muscle fibers. *Neuroscience* 2002; 109: 389–399.
24. Cairns BE, Svensson P, Wang K, Hupfeld S, Graven-Nielsen T, Sessle BJ, Berde CB, Arendt-Nielsen L. Activation of peripheral NMDA receptors contributes to human pain and rat afferent discharges evoked by injection of glutamate into the masseter muscle. *J Neurophysiol* 2003; 90: 2098–2105.
25. Svensson P, Cairns BE, Wang K, Hu JW, Graven-Nielsen T, Arendt-Nielsen L, Sessle BJ. Glutamate-evoked pain and mechanical allodynia in the human masseter muscle. *Pain* 2003; 101: 221–227.
26. Cairns BE, Svensson P, Wang K, Castrillon E, Hupfeld S, Sessle BJ, Arendt-Nielsen L. Ketamine attenuates glutamate-induced mechanical sensitization of the masseter muscle in human males. *Exp Brain Res* 2006; 169: 467–472.
27. Linher-Melville K, Haftchenary S, Gunning P, Singh G. Signal transducer and activator of transcription 3 and 5 regulate system Xc- and redox balance in human breast cancer cells. *Mol Cell Biochem* 2015; 405: 205–221.
28. Smith QR. Transport of glutamate and other amino acids at the blood-brain barrier. *J Nutr* 2000; 130: 1016S–1022S.
29. Dixon WJ. Efficient analysis of experimental observations. *Annu Rev Pharmacol Toxicol* 1980; 20: 441–462.

30. Zhu YF, Henry JL. Excitability of Aβ sensory neurons is altered in an animal model of peripheral neuropathy. *BMC Neurosci* 2012; 13: 15.

31. Zhu YF, Wu Q, Henry JL. Changes in functional properties of A-type but not C-type sensory neurons in vivo in a rat model of peripheral neuropathy. *J Pain Res* 2012; 5: 175–192.

32. Zhu YF, Kwiecien JM, Dabrowski W, Ungard R, Zhu KL, Huizinga JD, Henry JL, Singh G. Cancer pain and neuropathic pain are associated with A β sensory neuronal plasticity in dorsal root ganglia and abnormal sprouting in lumbar spinal cord. *Mol Pain* 2018; 14: 1744806918810099.

33. Jimenez-Andrade JM, Mantyh WG, Bloom AP, Xu H, Ferng AS, Dussor G, Vanderah TW, Mantyh PW. A phenotypically restricted set of primary afferent nerve fibers innervate the bone versus skin: therapeutic opportunity for treating skeletal pain. *Bone* 2010; 46: 306–313.

34. Peters CM, Ghilardi JR, Keyser CP, Kubota K, Lindsay TH, Luger NM, Mach DB, Schwei MJ, Sevcik MA, Mantyh PW. Tumor-induced injury of primary afferent sensory nerve fibers in bone cancer pain. *Exp Neurol* 2005; 193: 85–100.

35. Hald A, Nedergaard S, Hansen RR, Ding M, Heegaard A-M. Differential activation of spinal cord glial cells in murine models of neuropathic and cancer pain. *Eur J Pain Lond Pain* 2009; 13: 138–145.

36. Honore P, Luger NM, Sabino MA, Schwei MJ, Rogers SD, Mach DB, O'keefe PF, Ramnaraine ML, Clohisy DR, Mantyh PW. Osteoprotegerin blocks bone cancer-induced skeletal destruction, skeletal pain and pain-related neurochemical reorganization of the spinal cord. *Nat Med* 2000; 6: 521–528.

37. Wall PD, Woolf CJ. Muscle but not cutaneous C-afferent input produces prolonged increases in the excitability of the flexion reflex in the rat. *J Physiol* 1984; 356: 443–458.

38. Woolf CJ. Evidence for a central component of post-injury pain hypersensitivity. *Nature* 1983; 306: 686–688.

39. Cairns BE, Dong X, Mann MK, Svensson P, Sessle BJ, Arendt-Nielsen L, McErlane KM. Systemic administration of monosodium glutamate elevates intramuscular glutamate levels and sensitizes rat masseter muscle afferent fibers. *Pain* 2007; 132: 33–41.

40. Bhave G, Karim F, Carlton SM, Gereau RW. Peripheral group I metabotropic glutamate receptors modulate nociception in mice. *Nat Neurosci* 2001; 4: 417–423.

41. Carlton SM, Coggeshall RE. Inflammation-induced changes in peripheral glutamate receptor populations. *Brain Res* 1999; 820: 63–70.

42. Carlton SM, Hargett GL, Coggeshall RE. Localization and activation of glutamate receptors in unmyelinated axons of rat glabrous skin. *Neurosci Lett* 1995; 197: 25–28.

43. Coggeshall RE, Carlton SM. Ultrastructural analysis of NMDA, AMPA, and kainate receptors on unmyelinated and myelinated axons in the periphery. *J Comp Neurol* 1998; 391: 78–86.

44. Walker K, Reeve A, Bowes M, Winter J, Wotherspoon G, Davis A, Schmid P, Gasparini F, Kuhn R, Urban L. mGlu5 receptors and nociceptive function II. mGlu5 receptors functionally expressed on peripheral sensory neurones mediate inflammatory hyperalgesia. *Neuropharmacology* 2001; 40: 10–19.

45. Cairns BE, Gambarota G, Dunning PS, Mulkern RV, Berde CB. Activation of peripheral excitatory amino acid receptors decreases the duration of local anesthesia. *Anesthesiology* 2003; 98: 521–529.

46. Ro JY. Contribution of peripheral NMDA receptors in craniofacial muscle nociception and edema formation. *Brain Res* 2003; 979: 78–84.

47. Sato K, Kiyama H, Park HT, Tohyama M. AMPA, KA and NMDA receptors are expressed in the rat DRG neurones. *Neuroreport* 1993; 4: 1263–1265.

48. Bardoni R. Role of presynaptic glutamate receptors in pain transmission at the spinal cord level. *Curr Neuropharmacol* 2013; 11: 477–483.

49. Chiechio S, Caricasole A, Barletta E, Storto M, Catania MV, Copani A, Vertechy M, Nicolai R, Calvani M, Melchiorri D, Nicoletti F. L-Acetylcarnitine induces analgesia by selectively up-regulating mGlu2 metabotropic glutamate receptors. *Mol Pharmacol* 2002; 61: 989–996.

50. Chiechio S, Zammataro M, Morales ME, Busceti CL, Drago F, Gereau RW, Copani A, Nicoletti F. Epigenetic modulation of mGlu2 receptors by histone deacetylase inhibitors in the treatment of inflammatory pain. *Mol Pharmacol* 2009; 75: 1014–1020.

51. Cabral GA, Griffin-Thomas L. Emerging role of the CB2 cannabinoid receptor in immune regulation and therapeutic prospects. *Expert Rev Mol Med* 2009; 11: e3.